A MATLAB Platform for Characterizing MIMO-OFDM Communications with Software-Defined Radios

Ryan Measel, Donald J. Bucci, Christopher S. Lester, Kevin Wanuga
Richard Primerano, Kapil R. Dandekar, and Moshe Kam

Department of Electrical and Computer Engineering
Drexel University, Philadelphia, PA 19104

***Abstract*—A new MATLAB-based, wireless measurement platform using an existing software-defined radio architecture is presented. It augments IEEE 802.11g MIMO-OFDM physical layer schemes with new designs such as Maximal Ratio Combining, Alamouti coding, and Spatial Multiplexing. The platform provides a series of metrics, including channel capacity, Error Vector Magnitude (EVM), and Post-Processing Signal-to-Noise Ratio (PP-SNR) to characterize link and network performance. The software implementation and test protocol of the platform are presented with a validation study demonstrating its application.**

I. Introduction

Wireless networks operate in many environments with different electromagnetic characteristics. Some "typical" environments, such as office, residential, and urban spaces, have been modeled for the purposes of simulating wireless communications (e.g., [1]) across various physical layers and coding methods. More challenging RF environments exist that have not been addressed by the standard wireless design libraries. For example, below-deck spaces on naval vessels [2] and certain industrial facilities [3] exhibit high multipath interference and frequency selectivity that require special considerations.

In order to characterize network performance in these "special" environments, channel and link level metrics are needed which are not routinely available on consumer-grade hardware. Specialized, professional equipment is often used in such circumstances requiring considerable investment in hardware and logistics. There is a clear need for a lightweight, mobile test platform which is capable of performing a more comprehensive characterization of wireless communications than what is available now.

Measurement platforms that incorporate Software-Defined Radios (SDR) are a viable option to address this need. SDRs have a small, lightweight form factor, and they can be used in physically constrained locations and in conjunction with mobile applications. They are also relatively inexpensive. Several SDR implementations [4, 5] have been proposed, though they appear limited to specific physical layer schemes and applications. These systems typically run off of FPGAs and require user knowledge of embedded systems programming.

A MATLAB-based SDR platform is presented here for the direct characterization of Multi-Input, Multi-Output (MIMO)-Orthogonal Frequency Division Multiplexing (OFDM) communications in most environments. The platform has a modular subsystem design that implements a MIMO-OFDM wireless network with one of four physical layer schemes similar to IEEE 802.11g: Single-Input-Single-Output (SISO), 1×2 Maximal Ratio Combining (MRC), 2×2 Alamouti code, and 2×2 Spatial Multiplexing (SMUX). The current version of the platform uses the *Wireless Open-Access Research Platform (WARP)* v3 SDR [6], although its modular nature would allow it to employ any SDR with appropriate buffer access. Data is OFDM-encoded and decoded based on the specified physical layer scheme entirely within MATLAB. The raw receive data can be used to derive a variety of desired channel and link-level metrics, including channel capacity, Error Vector Magnitude (EVM), and Post-Processing Signal-to-Noise Ratio (PP-SNR).

A measurement validation study was performed aboard the decommissioned *Ticonderoga*-class cruiser, *Thomas S. Gates* (CG 51). The study made use of the measurement platform and test protocol described in this document. Performance metrics were extracted from the measurements and used for analysis of wireless communication in the ship environment. We use the validation study to demonstrate the capabilities of the proposed measurement platform.

This paper is organized as follows: In Section II, the MATLAB OFDM subsystems, implemented physical layer schemes, and WARP v3 SDR are described. The performance metrics are discussed in Section III. Section IV contains the test protocol. The measurement validation study performed aboard the *Thomas S. Gates* is presented in Section V.

II. Measurement Platform Implementation

A. Packet Structure

This implementation of the OFDM packet structure is similar to IEEE 802.11g [7]. A packet contains 30 OFDM words and each word contains 64 subcarriers. Four of the subcarriers are reserved for pilot tones, which are used in frequency offset correction of channel estimates [7, Expression

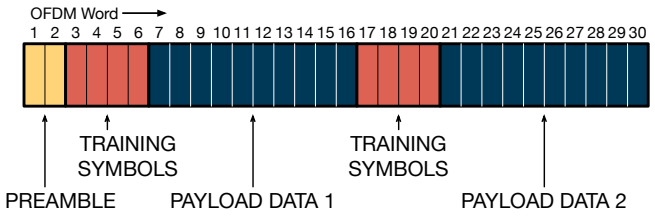

Fig. 1. Diagram illustrating the structure of a packet with 30 OFDM words. The first two OFDM words contain the preamble. The remaining 28 words alternate between four OFDM words dedicated to training data and 10 words for the data payload.

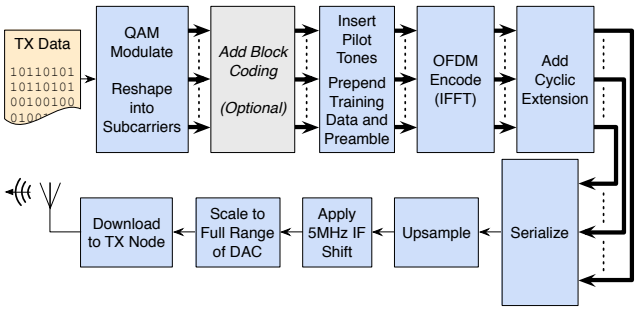

Fig. 2. Block diagram of the OFDM transmitter subsystem

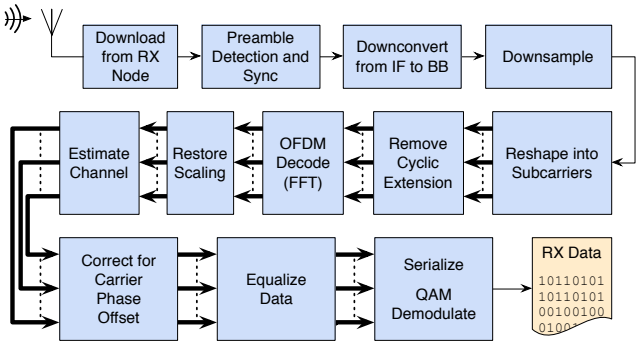

Fig. 3. Block diagram of the OFDM receiver subsystem

18–25]. Twelve of the subcarriers are set to null as in [7, Figure 18–3], and the remaining 48 subcarriers contain data.

A packet is comprised of three types of blocks: *preamble*, *training symbols*, and *data*. The preamble block has two IEEE 802.11 long OFDM training symbols [7, Section 18.3.3], which are used for timing synchronization and packet detection. The training symbols block has four OFDM words. Two of the four OFDM words are arbitrary BPSK streams used to estimate Channel State Information (CSI). The remaining two OFDM words are null, to prevent beamforming when estimating the channel coefficients for MIMO physical layer schemes. The data block contains 10 OFDM words filled with randomly generated data.

Due to the time varying nature of the channel, a trade-off exists between the length of a data block and the validity of the CSI. Long data blocks can have stale CSI that causes carrier frequency offset, while short data blocks incur more overhead and require more packet transmissions. Since all the processing on this platform is done in software, there is a large delay (on the order of hundreds of milliseconds) between packet transmissions. While a slow rate of transmission does not affect the results, it does increase the length of the test.

A method was developed to decrease the testing time of the platform. The training symbols and data payload are duplicated and concatenated into a single packet as shown in Fig. 1. A total of 20 OFDM words (960 symbols) of data is sent per transmission. The overhead is slightly increased with the inclusion of the second set of training symbols, but the higher data payload transmission rate vastly reduces the testing time without sacrificing the integrity of the data.

B. Transmitter Subsystem

Fig. 2 shows the OFDM transmission subsystem for a single transmission stream. The data is QAM modulated first and then reshaped into the 48 OFDM data subcarriers. The subcarriers are then encoded if required by the specified physical layer (e.g., Alamouti code). The pilot tones are inserted according to [7, Section 18.3.5.9]. In the MIMO cases, the pilot tones are interleaved in space and time (i.e., across subcarriers and OFDM words) to prevent deconstructive combining [8, Section 3.6]. The training symbols and preamble OFDM words are placed in front of the data/pilot tone OFDM words. The entire packet is then OFDM-encoded via a 64 point IFFT, producing the OFDM waveforms for each word. For the second set of training symbols and data payload, the first set is repeated and appended to the OFDM packet. A guard interval consisting of a 16 sample cyclic prefix is added to each OFDM waveform, increasing the size of the OFDM word to 80 samples. After serializing the OFDM waveforms, the entire packet is upsampled by a factor of 4 to reduce the bandwidth to 10 MHz. The packet is upconverted to an IF of 5 MHz to prevent attenuation near DC. Finally, the preamble, training data, and data payload waveforms are individually scaled to the dynamic range of the WARP D/A and A/D converters to ensure maximum resolution in quantization while preventing clipping.

C. Receiver Subsystem

Fig. 3 shows the general OFDM receiver subsystem. For each reception, the raw received data plus an additional 300 samples are downloaded from the WARP nodes. The additional 300 samples act as a synchronization buffer to ensure that sufficient samples are downloaded to synchronize the transmission. Packet detection and synchronization occur via cross correlating the known preamble sequence (a single IEEE 802.11 long training symbol) with the received data. A packet is considered detected if the largest cross correlation magnitude is greater than a prespecified threshold.

After synchronization, the stream is downconverted to baseband and downsampled by a factor of 4. The entire packet is reshaped into subcarriers, and the cyclic extension guard interval is removed. The OFDM words are then recovered from the OFDM waveforms by performing a 64 point FFT. The

channel coefficients are estimated from the training symbols. The carrier phase offset for each OFDM word is estimated using the dedicated pilot tones as in [9, Equation 8.17] and corrected by applying an inverse phase shift. The data payload is equalized using the channel estimates according to the specified physical layer, after which the received QAM symbols are serialized and demodulated.

D. Physical Layer Schemes

The platform currently implements four (4) OFDM physical layer schemes: Single-Input-Single-Output (SISO), 1×2 Maximal Ratio Combining (MRC), 2×2 Alamouti code, and 2×2 spatial multiplexing via Vertical Bell Labs Layered Space-Time Architecture (VBLAST). In the SISO scheme, the channel coefficients of each OFDM subcarrier are used to equalize the subcarriers of the OFDM packet. In 1×2 MRC, the signals from each receive antenna are weighted according to their individual SNRs and then summed. The weights are formed in terms of the channel coefficients for each subcarrier, as in [10, Chapter 7]. In the 2×2 Alamouti code, the data is split into two separate streams at the transmitter node and redundancy is added in the form of orthogonal representations of the data [11]. Finally, a 2×2 spatial multiplexing scheme is implemented via the VBLAST algorithm [12] which splits the transmitted data across two streams. At the receiver, the streams are decoded using a combination of linear nulls and symbol cancellation at each OFDM subcarrier.

E. WARP v3 Software-Defined Radio

The WARP v3 Kit is a SDR platform developed by Rice University and Mango Communications [6]. It is built on a Xilinx Virtex-6 LX240T FPGA with two programmable RF interfaces operating at 2.4 and 5 GHz with a 40 MHz bandwidth. The WARP v3 Kit was selected for use with the platform due to its accessibility and ease of interface with MATLAB. The WARPLab 7.1 reference design is a buffer-based design with no physical or MAC layer which allows for their implementation in software. The reference design was used as a starting point to develop the measurement platform. The generated transmit waveforms are sent directly to the transmit buffers and the received waveforms are extracted directly from the receive buffer. Modulation, coding, and equalization are performed in MATLAB.

III. Performance Metrics

The received data is converted first into raw IQ, decoded IQ, and finally demodulated IQ. The CSI is estimated using the received training symbols. Several channel and link level metrics can be derived from the data in each of these states. A subset of the possible metrics was selected to analyze the measurement study in Section V:

1) **Channel Capacity** is the upper bound on the rate of information that can be sent over a channel with an arbitrarily small level of error. It illustrates the effects of changing channel conditions on throughput. In this system, channel capacity is calculated (in bits per Hertz) on a per packet basis from the normalized channel gain estimates recovered in each 802.11 packet. MIMO-OFDM Channel capacity is defined as a function of CSI and SNR. The physical interpretation of the SNR is dependent on the channel normalization employed [13].
2) **Error Vector Magnitude (EVM)** is the Euclidean distance between a transmitted and a received IQ symbol. The distribution of the EVM is an indicator of link performance.
3) **Post-Processing Signal-to-Noise Ratio (PP-SNR)** is the ratio (expressed in dB) of signal power to the RMS EVM and serves as a measure of the signal integrity. It is calculated as Root Mean Square average of all symbols in all test transmissions. PP-SNR is similar to SNR, but includes sources of error such as non-linear distortion in the radio transceiver, error in channel estimation, and noise enhancement from equalization.

IV. Test Protocol

A test protocol which uses the SDR platform is outlined below. Prior to the start of the test, the gains on each transmitting port are normalized to allow for unbiased comparisons between single-input and multiple-input transmission schemes. An Agilent U2001H USB Power sensor was used to measure the output power. The transmit gains were adjusted accordingly to match output power. When multiple physical layer schemes are being compared, the transmissions of the different schemes are interleaved to improve the correlation between channels and reduce the effect of time variance. The test protocol is as follows:

1) Configure the node topology.
2) Calibrate the transmitter.
    a) Select a gain and send a SISO transmission.
    b) Repeat (2.a) until the PP-SNR is maximized without exhibiting gain saturation [14].
    c) Measure the transmit power of the transmitting port with a power sensor.
    d) Adjust the gain on the additional transmitting port to match the calibrated output power. If saturation occurs, repeat 2.a with a lower initial gain.
3) Execute the test.
    a) Send a SISO transmission (SISO/MRC).
    b) Receive the SISO transmission on both antennas.
    c) Send a MIMO transmission (Alamouti code/SMUX).
    d) Receive the MIMO transmission on both antennas.
    e) Repeat (3.a-b) for the desired number of trials.

Both SISO and MRC can be decoded from a SISO transmission (Step 3.a), since a copy of the transmitted signal is received on both receiver antennas. SISO decoding only uses a single RX stream, while MRC decoding uses both streams. Similarly, both Alamouti code and SMUX can be decoded from a MIMO transmission (Step 3.b) when the Alamouti encoding has been applied to both transmitted streams. For

SMUX decoding, the two streams are interpreted as independent data streams, ignoring that they contain an Alamouti block code. By decoding all four physical layer schemes using only two transmissions, the total number of transmissions (and length of the test) is halved.

V. Measurement Validation Study

A measurement campaign was completed using the SDR platform aboard the decommissioned *Ticonderoga*-class cruiser, *Thomas S. Gates* (CG 51) [15], at the Philadelphia Naval Yard. Currently, most on-ship communications in naval vessels are connected over hardwired networks, which have higher infrastructure costs and less flexibility than wireless networks. The objective of the campaign was to characterize wireless communication in the below-deck environment and determine the feasibility of implementing a wireless network there.

One of the environments tested during the campaign was a corridor that ran the length of the vessel. The corridor was selected as a prime location for the installation of core network infrastructure. A two node topology was deployed with a transmitter at the end of the corridor and a receiver 25.9 meters down the corridor through two watertight doors (Fig. 4). Both nodes were outfitted with two commercial, off-the-shelf dual band (2.4/5.8 GHz) omnidirectional antennas. One test was conducted with both doors open, and another was conducted with the door closed at the 11m mark.

In each test, a series of 500 transmissions was completed for each physical layer scheme. Each transmitted stream contains 960 symbols for a total of $9.6 * 10^5$ symbols per test.

The empirical Cumulative Distribution Functions (Figs. 5–9) of the EVM provide insights on the comparison of physical layer schemes and the effect of the door being closed. The level of link degradation is indicated by increased variance and heavy tails of the EVM distributions when the door is closed. Since the signal cannot penetrate the bulkhead, it must propagate through apertures in and around the watertight door, including a rubber gasket and a glass porthole.

The signal integrity for all physical layer schemes with the door open and closed is displayed in Fig. 7. The two diversity schemes, MRC and Alamouti code, outperform SISO and SMUX in both cases as expected. Since Alamouti code and MRC have similar PP-SNR when the door is closed, it is probably that one of the Alamouti code transmit streams is severely degraded (likely by the door) which negates the benefits of the transmitter diversity. Closing the door resulted in approximately 5 dB of loss for SISO, MRC, and Alamouti code and about 8 dB for SMUX.

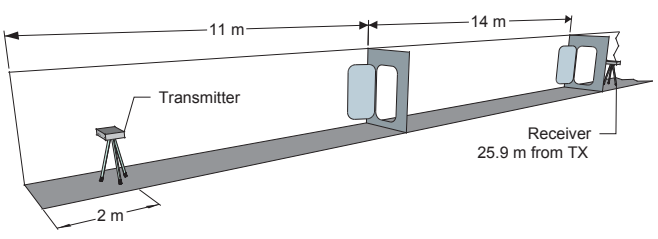

Fig. 4. Cross section of the corridor test environment with node topology on *Thomas S. Gates* (CG 51).

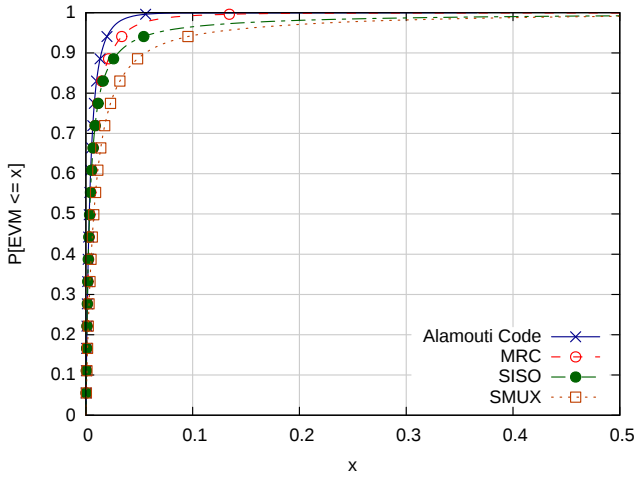

Fig. 5. Empirical Cumulative Distribution Function for the EVM of physical layer schemes with the door open

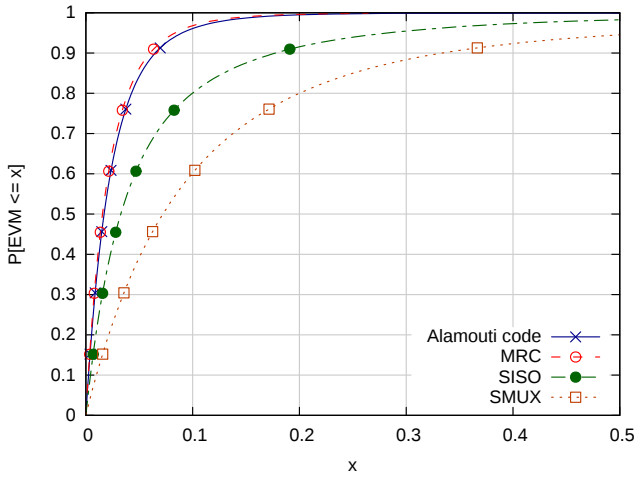

Fig. 6. Empirical Cumulative Distribution Function for the EVM of physical layer schemes with the door closed

The channel capacity of the physical layer schemes is shown in Figs. 8–9. The observed CSI is normalized such that the horizontal axis shows the mean received SNR per receiver from all transmitters [13]. The capacity for an Independent, Identically Distributed (IID) channel is presented for comparison. The IID capacity represents the upper bound of the capacity in a MIMO link of equal channel gain. SMUX has the highest capacity of all the physical layer schemes. Since the CSI is normalized, SMUX should have the highest capacity, because it is transmitting at twice the rate of the other schemes. Alamouti code and MRC both outperform SISO by a minimum of 24% due to the added transmit and receiver diversity. Somewhat surprisingly, the capacity increases for all four schemes when the door is closed. In this case, less energy

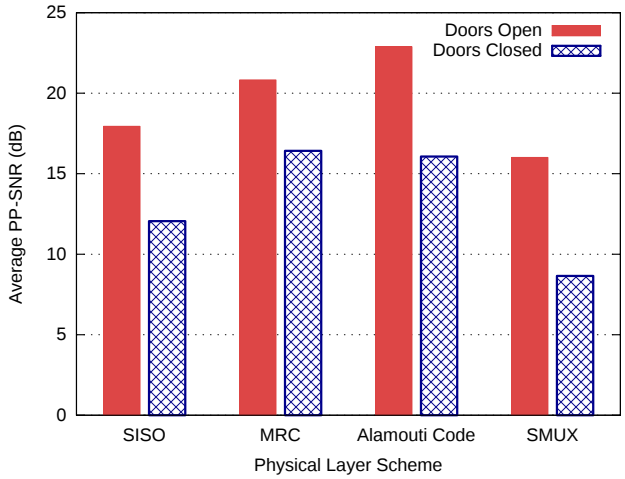

Fig. 7. PP-SNR of physical layer schemes with both the door open and closed

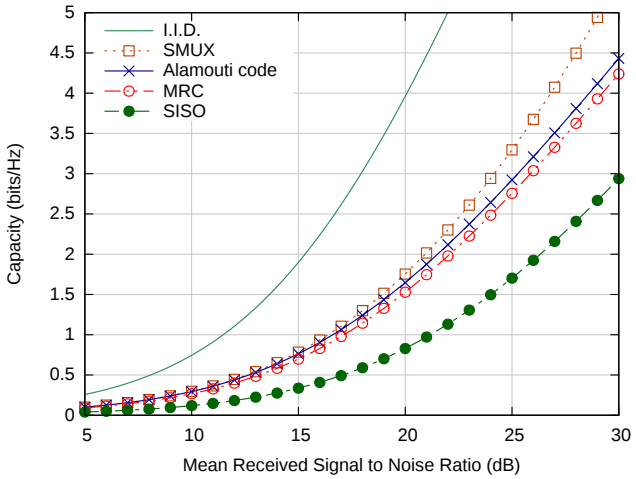

Fig. 9. Channel capacity for physical layer schemes with the door closed

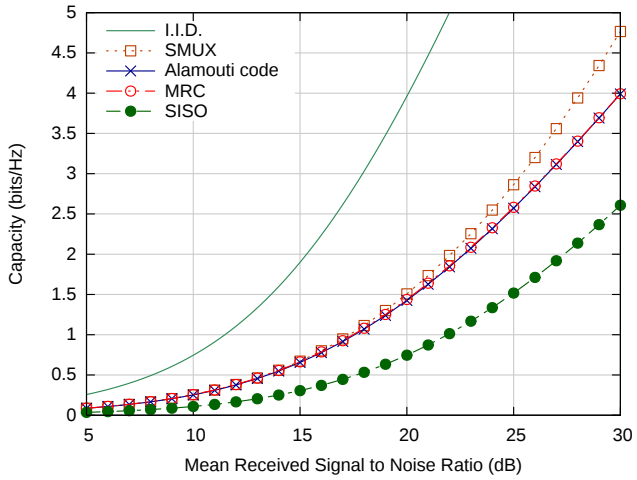

Fig. 8. Channel capacity for physical layer schemes with the door open

couples into the cavity with the receiver, which decreases the multipath interference characteristic of a highly reverberant environment. This trend indicates that the channel may become less frequency selective when the door is closed.

VI. Conclusions

Consumer-grade equipment is incapable of performing detailed analysis of wireless communications in certain challenging environments. Specialized equipment for these environments is often cost prohibitive and not suited for mobile applications and field testing. A MATLAB-based SDR platform was presented as a cost-effective, lightweight alternative. The platform implements four MIMO-OFDM transmission schemes based on the IEEE 802.11g protocol and allows full user access to transmit and receive buffers. The raw data extracted from the platform can be used to derive a host of metrics necessary for evaluation of channel and link properties. A measurement validation study aboard a decommissioned naval vessel was presented. It demonstrated the SDR platform's ability to characterize a challenging wireless environment without having to move large, expensive, and fragile equipment below the decks of the vessel.

Acknowledgment

The authors thank the staff at the Philadelphia, PA, Naval Inactive Ship Maintenance Facility for their assistance in navigating *Thomas S. Gates*. This study was supported in part by the Office of Naval Research (award N00014–13–1–0312) and the National Science Foundation (grants CNS-0854946 and CNS-0923003).

References

[1] V. Erceg *et al.*, "TGn channel models," IEEE, Garden Grove, California, USA, Tech. Rep. P802.11, Jun. 2004.

[2] E.L. Mokole, M. Parent *et al.*, "RF propagation on ex-*USS Shadwell*," in *Proc. IEEE-APS Conf. Antennas and Propagation for Wireless Commun.*, 2000, pp. 153–156.

[3] P. Angskog, C. Karlsson *et al.*, "Sources of disturbances on wireless communication in industrial and factory environments," in *Proc. Asia-Pacific Symp. on Electromagnetic Compatibility*, 2010.

[4] K. Mandke, S.H. Choi *et al.*, "Early results on Hydra: A flexible MAC/PHY multihop testbed," in *Proc. IEEE Veh. Technology Conf.*, 2007, pp. 1896–1900.

[5] P. Murphy, F. Lou *et al.*, "An FPGA based rapid prototyping platform for MIMO systems," in *Proc. Asilomar Conf. on Signals, Syst. and Comput.*, vol. 1, 2003, pp. 900–904.

[6] Rice University, "Wireless Open-Access Research Platform." [Online]. Available: http://warp.rice.edu

[7] *Inform. Technology—Telecommun. and Inform. Exchange Between Syst.—Local and Metropolitan Area Networks—Specific Requirements—Part 11: Wireless LAN Medium Access Control (MAC) and Physical Layer (PHY) Specifications*, IEEE Std. 802.11-1997.

[8] P.O. Murphy, "Design, implementation, and characterization of a cooperative communications system," Ph.D. dissertation, Rice University, Dec. 2010.

[9] M. Jankiraman, *Space-time codes and MIMO systems*. Artech House, Inc., 2004.

[10] R. Janaswamy, *Radiowave Propagation & Smart Antennas for Wireless Communications*. Kluwer Academic Publishers, 2000.

[11] S.M. Alamouti, "A simple transmit diversity technique for wireless communications," *IEEE J. Sel. Areas Commun.*, vol. 16, pp. 1451–1458, Oct. 1998.

[12] P.W. Wolniansky, G.J. Foschini *et al.*, "V-BLAST: An architecture for realizing very high data rates over the rich-scattering wireless channel," in *Proc. URSI Int. Symp. on Signals, Syst., and Electronics*, 1998, pp. 295–300.

[13] S. Loyka and G. Levin, "On physically-based normalization of MIMO channel matrices," *IEEE Trans. Wireless Commun.*, vol. 8, no. 3, pp. 1107–1112, Mar. 2009.

[14] F. Da Ros, R. Borkowski *et al.*, "Impact of gain saturation on the parametric amplification of 16-qam signals," in *Proc. Conf. on Optical Commun.*, 2012, pp. 1–3.

[15] Naval Historical Society. (2005, Nov.) USS *Thomas S. Gates* (CG-51). Department of the Navy. 805 Kidder Breese St. SE, Washington Navy Yard, Washington, DC, USA. [Online]. Available: http://www.history.navy.mil/danfs/t4/thomas_s_gates.htm